Inorganic Chemistry

ARTICLE

pubs.acs.org/IC

Synthesis of Phase-Pure Interpenetrated MOF-5 and Its Gas Sorption Properties

Hyunuk Kim,[†] Sunirban Das,[†] Min Gyu Kim,[‡] Danil N. Dybtsev,[§] Yonghwi Kim,[†] and Kimoon Kim*[,†,§]

[†]National Creative Research Initiative Center for Smart Supramolecules, Department of Chemistry, [§]Division of Advanced Materials Science, and [‡]Pohang Accelerator Laboratory, Pohang University of Science and Technology, San 31 Hyojadong, Pohang 790-784, Republic of Korea

Supporting Information

ABSTRACT: For the first time, phase-pure interpenetrated MOF-5 (**1**) has been synthesized and its gas sorption properties have been investigated. The phase purity of the material was confirmed by both single-crystal and powder X-ray diffraction studies and TGA analysis. A systematic study revealed that controlling the pH of the reaction medium is critical to the synthesis of phase-pure **1**, and the optimum apparent pH (pH*) for the formation of **1** is 4.0−4.5. At higher or lower pH*, $[Zn_2(BDC)_2(DMF)_2]$ (**2**) or $[Zn_5(OH)_4(BDC)_3]$ (**3**), respectively, was predominantly formed. The pore size distribution obtained from Ar sorption experiments at 87 K showed only one peak, at ∼6.7 Å, which is consistent with the average pore size of **1** revealed by single crystal X-ray crystallography. Compared to MOF-5, **1** exhibited higher stability toward heat and moisture. Although its surface area is much smaller than that of MOF-5 due to interpenetration, **1** showed a significantly higher hydrogen capacity (both gravimetric and volumetric) than MOF-5 at 77 K and 1 atm, presumably because of its higher enthalpy of adsorption, which may correlate with its higher volumetric hydrogen uptake compared to MOF-5 at room temperature, up to 100 bar. However, at high pressures and 77 K, where the saturated H_2 uptake mostly depends on the surface area of a porous material, the total hydrogen uptake of **1** is notably lower than that of MOF-5.

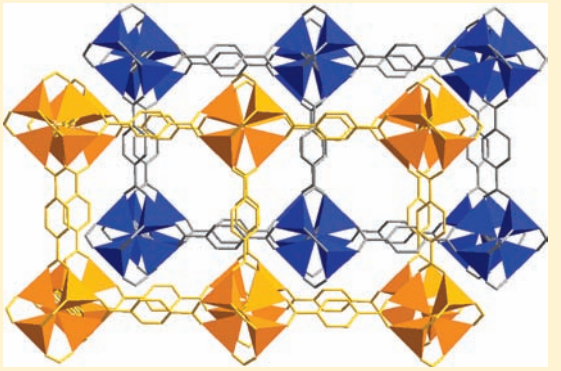

INTRODUCTION

During the past decade, great efforts have been devoted to the design of metal organic frameworks (MOFs)[1] with specific pore sizes, shapes, and chemical environments for applications in gas storage and separation, catalysis, magnetism, luminescence, and drug delivery.[2] Framework interpenetration,[3] by which the pores of one framework are intergrowned by one or more independent frameworks, is a commonly observed phenomenon in MOFs. While it may be a negative phenomenon from the gas storage point of view, because it significantly reduces the available void space, the interpenetration bears positive effects, including enhanced framework stability, increased heat of adsorption, and size selectivity.[4] Although a few examples have been recently reported,[5] the control of interpenetration is still quite challenging.[6]

MOF-5, one of the most studied MOFs prepared from Zn ions and 1,4-benzene dicarboxylic acid (H_2BDC), has a primitive cubic topology, composed of 6-connected tetranuclear $\{Zn_4O\}$ clusters at the vertices and BDC ligands as linkers.[7] After the first report of the structure, MOF-5 has been extensively investigated for gas storage, in particular, H_2 storage for applications in fuel cells.[8] Nevertheless, the reported gas sorption properties of MOF-5 showed substantial variations,[9] which has been attributed, at least in part, to the presence of organic and inorganic species in the pores.[10] Especially, it was discovered that MOF-5 could be often contaminated with a small amount of interpenetrated MOF-5 (**1**) with a doubly interpenetrated primitive cubic network.[10] Although the structure of **1** was reported,[10] the bulk properties of **1** have never been studied, as the synthesis of phase-pure **1** has been quite elusive so far. Herein, we report, for the first time, the synthesis of phase-pure **1**, as well as its stability and gas sorption properties. This systematic study demonstrates that controlling the pH[11] of the reaction media is a key to the successful synthesis of phase-pure **1**, which has not been widely recognized in the synthesis of porous MOFs.[12]

RESULTS AND DISCUSSION

Synthesis and Crystal Structure Determination. Solvothermal reaction of $Zn(NO_3)_2 \cdot 6H_2O$ and H_2BDC in DMF in the presence of *melamine* at 110 °C produced crystalline **1**. Single-crystal X-ray diffraction (XRD) analysis revealed that **1** has the same cubic topology as MOF-5 with 2-fold interpenetration (see Figure 1).[13] The interpenetrated framework **1** has two types of pores, with slightly different internal diameters (7.6 and 6.0 Å), because of the tilted BDC linkers connecting adjacent $\{Zn_4O\}$ oxoclusters (see Figure S1 in the Supporting Information).

Received: January 10, 2011
Published: March 17, 2011

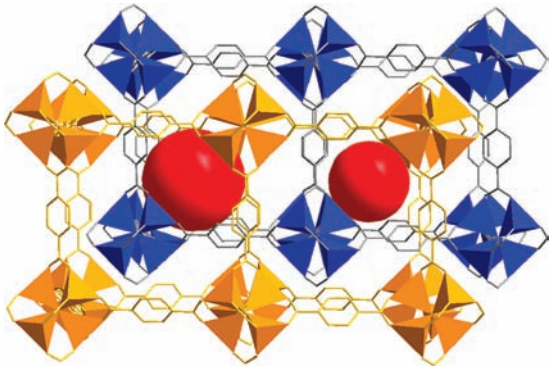

Figure 1. X-ray crystal structure of **1** with two types of pores (internal diameters = 7.6 and 6.0 Å).

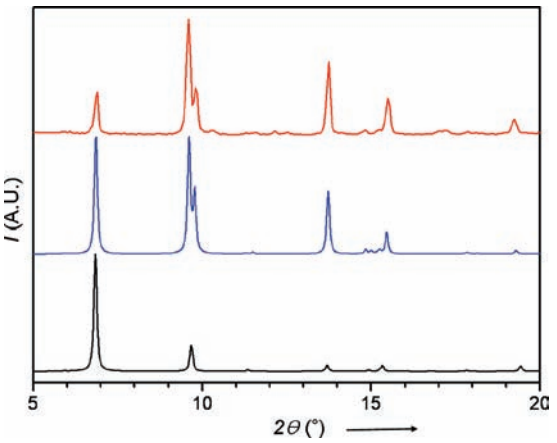

Figure 2. Powder X-ray diffraction (PXRD) patterns for as-synthesized **1** (red line), simulated **1** (blue line), and MOF-5 (black line).

Despite the 2-fold interpenetration, the solvent-accessible volume for **1** was estimated to be 49%, which is large enough for the inclusion of guest molecules.[14] Although melamine was present in the reaction medium, only dimethylformamide (DMF) and water molecules were included in the pores, which has been unequivocally confirmed by elemental analysis, as well as ^{1}H NMR and ^{13}C NMR spectroscopy, after digesting as-synthesized **1** in NaOH/D_2O (see Figure S2 in the Supporting Information). However, the same reaction solution without melamine produced a complicated mixture of crystalline products (see Figure S3 in the Supporting Information). Also, as described below, phase-pure **1** can be synthesized by adjusting the pH* value of the reaction medium between 4 and 4.5, instead of adding melamine into the reaction mixture.

Characterization of the Phase Purity. The phase purity of **1** was confirmed by powder X-ray diffraction (PXRD) analysis on a bulk sample. The PXRD profile of as-synthesized **1** well matched the simulated one, based on the single-crystal X-ray structure. Most notably, as-synthesized **1** exhibits two discrete peaks, at 2θ = 9.6° and 9.8°, whereas noninterpenetrated MOF-5 shows only one peak, at 9.7° (see Figure 2). As expected, **1** has higher thermal stability than MOF-5. Thermogravimetric analysis (TGA) showed that the interpenetrated framework decomposes above 450 °C, whereas MOF-5 starts to decompose at 400 °C (see Figure 3), which is consistent with the temperature-dependent PXRD study showing that **1** maintains its crystallinity up to

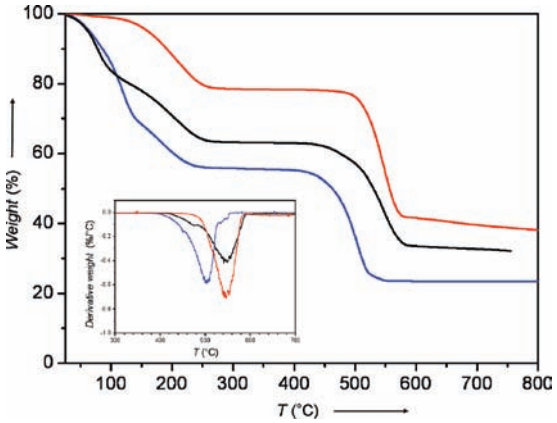

Figure 3. TGA data of **1** (red line), MOF-5 (blue line), and a physical mixture (50:50 wt %) of **1** and MOF-5 (black line). The inset represents the derivative weight loss of these materials.

430 °C (see Figure S4 in the Supporting Information). A close inspection of the derivative weight loss revealed practically no weight loss in the range of 400−450 °C for as-synthesized **1**, indicating no or little contamination of MOF-5 in the bulk sample of **1**.[15] Furthermore, guest-free **1** shows higher stability toward airborne moisture than noninterpenetrated MOF-5, because the crystallinity of the former remains intact for 5 days, while the latter decomposes after 1 day under the same conditions (see Figure S6 in the Supporting Information).[9]

Role of Melamine. Having discovered the synthesis of phase-pure **1**, we decided to investigate the role of melamine in the formation of an interpenetrated framework. We first eliminated the possibility of melamine acting as a template, because (1) melamine is not included in the final product (**1**), and (2) the same reaction in the presence of other organic additives such as aniline and 2,4,6-tris(4-pyridyl)-1,3,5-triazine also produced phase-pure **1**, as confirmed by PXRD and TGA (see Figures S7 and S8 in the Supporting Information); the tris-pyridyl-triazine is certainly too large to be included in the micropores of **1**. It then occurred to us that these organic additives, including melamine, might behave as weak organic bases to affect the pH of the reaction medium. Considering that the same reaction solution without these organic bases produced a complicated mixture of crystalline products (see Figures S3 and S9 in the Supporting Information), these results suggested that controlling the pH of the reaction medium is critical in the synthesis of phase-pure **1**.

pH Dependence of the Synthesis of 1. To better understand the effect of the pH of the reaction medium on the synthesis of the crystalline products, we carried out a systematic study. In this study, however, the true pH of the reaction medium is difficult to define, because the major component of the solution is DMF. Following other people's work,[11] we therefore decided to use the pH* values of the solution, which were directly measured by a conventional pH meter equipped with a glass electrode. The pH* of a mixture of $Zn(NO_3)_2 \cdot 6H_2O$ (2.00 mmol) and H_2bdc (0.75 mmol) in DMF (15 mL) was measured to be 3.8. The pH* of the reaction mixture was adjusted in the range between 2.0 and 6.0,[11] by adding a small amount of aqueous NaOH (2.5 M) or HCl (2.5 M) solution.[16] After the reaction, the phase composition of resulting crystalline products was examined by PXRD and X-ray absorption spectroscopy. Interestingly, between pH* 4.0 and pH* 4.5, only crystalline phase **1** was observed (see Figure 4). Especially, highly crystalline, phase-pure interpenetrated phase **1** was

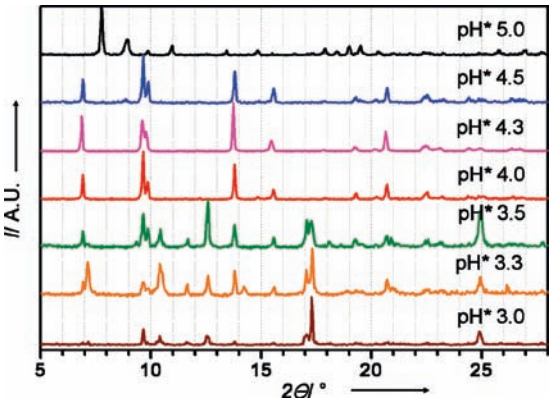

Figure 4. Powder X-ray diffraction (PXRD) spectra of crystalline materials obtained at different pH* values.

produced at pH* 4.3, which corresponds to the pH* of the reaction medium in the presence of melamine (see Figure S10 in the Supporting Information). When the pH* value of the solution was adjusted above 4.5 or below 4.0, other Zn(II)-terephthalate crystalline phases were identified in the solid product. In particular, at lower pH* ($\leq$3.5), the XRD pattern of the product was consistent with a simulated one for binuclear $[Zn_2(BDC)_2(DMF)_2]$ layered zinc(II) terephthlate $[Zn_2(BDC)_2(DMF)_2]$ (**2**).[17] At higher pH* ($\geq$5.0), the diffraction pattern of the product well matched that of $[Zn_5(OH)_4(BDC)_3]$ (**3**) phase.[17] Apparently, the addition of a base to the reaction mixture led to the formation of MOFs such as **1** or **3** that contained oxo- or hydroxo- polynuclear zinc(II) clusters. The X-ray absorption near edge structure (XANES) and extended X-ray absorption fine structure (EXAFS) spectra for the solid products obtained at pH* 3.0, 4.3, and 5.0 were consistent with the structures of the above-mentioned compounds with different local Zn environments (see Figure 5 and Figure S11 in the Supporting Information).

$$2Zn^{2+} + 2BDC^{2-} + 2DMF \rightarrow [Zn_2(BDC)_2(DMF)_2]\ (\mathbf{2}) \qquad pH^* \leq 3.5$$

$$4Zn^{2+} + 3BDC^{2-} + H_2O \rightarrow \frac{1}{2}[Zn_4O(BDC)_3]_2\ (\mathbf{1}) + 2H^+ \qquad 4 \leq pH^* \leq 4.5$$

$$5Zn^{2+} + 3BDC^{2-} + 4H_2O \rightarrow [Zn_5(OH)_4(BDC)_3]\ (\mathbf{3}) + 4H^+ \qquad pH^* \geq 5$$

EXAFS Study of the Reaction Mixture during the Reaction. Generally, the formation mechanism of MOFs still is not well understood. Few experimental study has been carried out to elucidate the formation mechanism of MOFs. Nevertheless, there was an EXAFS study revealing an intermediate metal cluster, which acts as a secondary building unit (SBU), in the reaction mixture during the formation of an MOF.[18] As a part of our effort to elucidate the mechanism of the formation of **1** and to understand the effect of pH on its formation, we therefore decided to monitor the reaction via EXAFS spectroscopy, to see if we could detect polynuclear Zn(II) intermediates such as $\{Zn_4(O)(BDC)_6\}$ or $\{Zn_2(BDC)_4\}$ in solution, which can act as SBUs of the final products. We carefully examined Zn(II) complexes formed during the reaction, especially at the early

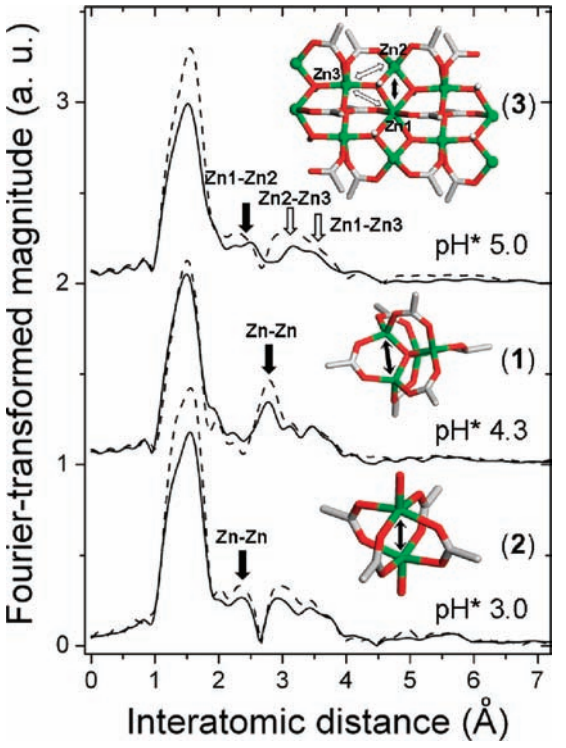

Figure 5. Normalized Zn K-edge Fourier-transformed magnitudes of k^2-weighted EXAFS spectra for solid products obtained at different pH* (pH* = 3.0, 4.3, and 5.0) (solid line) and known MOFs (dashed line). Reference compounds **3** and **2** were synthesized by reported methods,[17] and interpenetrated MOF-5 (**1**) was synthesized in the presence of melamine, as described in the text. Characteristic patterns of Zn−Zn interatomic correlations in the EXAFS spectra are marked by arrows.

stage of the reaction (up to 2.5 h) as crystalline products started to appear in 2 h. However, the EXAFS data of the reaction mixture at pH* 4.3 during the first 2.5 h of the reaction at 110 °C revealed only the mononuclear complex $[Zn(DMF)_6]^{2+}$ as a major component in the solution (see Figures S12 and S13 in the Supporting Information).[19] Similar EXAFS spectra were also obtained for the reaction mixtures at pH* 3.0 and 5.0 (see Figures S14 and S15 in the Supporting Information). Therefore, we concluded that polynuclear zinc(II) cluster intermediates exist, if any, only in low concentration in the solution, presumably because of low solubility and/or high reactivity.

Although the EXAFS study failed to reveal the multinuclear Zn(II) intermediates, we can speculate about a possible mechanism of formation for **1**. The addition of melamine (or NaOH solution) to a mixture of $Zn(NO_3)_2 \cdot 6H_2O$ and H_2bdc in DMF raises the pH* of the solution to ~4.3, at which both the deprotonation of terephthalic acid and water (see the chemical equation above), and the assembly of an oxo-bridged tetranuclear Zn(II) cluster $\{Zn_4O\}$ are strongly promoted to eventually produce zinc(II) oxo-terephthalate coordination network $[Zn_4O(BDC)_3]$. The initially formed $[Zn_4O(BDC)_3]$ coordination network acts as a template to facilitate the formation of another identical $[Zn_4O(BDC)_3]$ coordination network inside the pores of the template, resulting in the self-assembly of the doubly interpenetrated MOF-5 framework **1**. Once formed, the crystals of the doubly interpenetrated framework **1** continue to grow through the formation of BDC^{2-}-interlinked $\{Zn_4O\}$ complexes directly on the crystal surface under the solvothermal

dx.doi.org/10.1021/ic200054b |*Inorg. Chem.* 2011, 50, 3691–3696

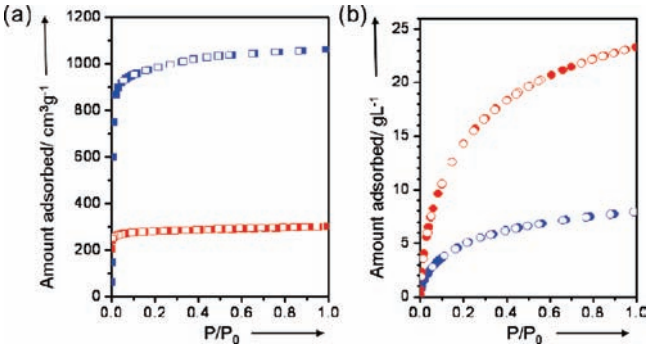

Figure 6. Nitrogen (squares) and hydrogen (circles) sorption isotherms of **1** (red) and MOF-5 (blue) at 77 K. (Solid symbols represent adsorption data, open symbols represent desorption data.)

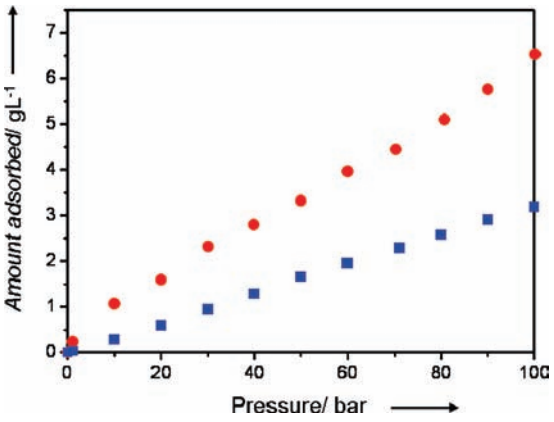

Figure 7. Hydrogen sorption isotherms of MOF-5 (squares) and **1** (circles) at 298 K.

conditions. At higher pH (pH* ≥5), the equilibrium is shifted toward the formation of MOFs containing a higher number of deprotonated water (OH^-) species per zinc(II) cation in the formula, such as **3** (see the chemical equation above).

Gas Sorption Properties. To investigate the gas sorption properties of **1**, the as-synthesized material was activated at 120 °C for 2 days. The nitrogen sorption isotherm for activated **1** at 77 K showed a typical type I behavior of microporous materials (Figure 6a). The Langmuir surface area of **1** estimated by nitrogen sorption isotherms is 1130 m^2/g, which is much smaller than that of MOF-5 (4400 m^2/g),[9] because of the smaller void space of **1**. The pore size distribution obtained from an Ar sorption experiment at 87 K showed only one peak, at ~6.7 Å (see Figure S16 in the Supporting Information), which is consistent with the average pore size of **1**.

Despite the much smaller surface area of **1**, compared to MOF-5, the hydrogen sorption capacity of **1** at 77 K and 1 atm is significantly higher than that of MOF-5.[20] The gravimetric hydrogen uptake of **1** at 1 atm and 77 K (2.0 wt %) is 54% higher than that of MOF-5 (see Figure S17 in the Supporting Information). For volumetric hydrogen uptake, this difference is even more pronounced: 23.3 g L^{-1} for **1** vs. 7.9 g L^{-1} for MOF-5 (at 1 atm and 77 K), because of the higher density of the framework of **1** (see Figure 6b).[21] The enthalpy of adsorption at zero coverage for **1**, estimated by the virial equation, using the H_2 sorption isotherms at 77 and 87 K, is 7.6 kJ/mol (see Figure S18 in the Supporting Information), which is much higher than that of MOF-5 (4.9 kJ/mol),[22] suggesting that the higher hydrogen sorption capacity of **1** at low pressure could be attributed to its higher enthalpy of adsorption. This may correlate with the observation that the volumetric hydrogen uptake of **1** at room temperature (RT) and 100 bar was twice as much as that of MOF-5, because of a higher Langmuir sorption constant, which, in turn, resulted from a higher sorption enthalpy (see Figure 7). At high pressures and 77 K, where the saturated H_2 uptake mostly depends on the surface area of a porous material,[23] however, the total hydrogen uptake of **1** (2.8 wt %, 33 g L^{-1} at 100 bar and 77 K) is notably lower than that of MOF-5 (10.0 wt %, 66 g L^{-1} at 100 bar and 77 K)[9] (see Figure S20 in the Supporting Information).

CONCLUSIONS

We have synthesized and characterized, for the first time, phase-pure interpenetrated MOF-5, **1**. A systematic study revealed that controlling the pH of the reaction medium is critical to the synthesis of phase-pure **1**, and the optimum pH* is 4.0−4.5 for the synthesis. At higher or lower pH*, other phases were predominantly formed. Interestingly, phase-pure **1** showed a much higher hydrogen capacity than MOF-5 at 77 K and 1 atm, presumably because of its higher enthalpy of adsorption, which may correlate with its higher volumetric hydrogen uptake, compared to MOF-5 at room temperature, up to 100 bar, even though the surface area of the former is much smaller than that of the latter. These results demonstrate that a careful pH control of reaction solution is critical for the synthesis of phase-pure porous MOFs, where impurities greatly affect the properties of materials, such as gas sorption.

EXPERIMENTAL SECTION

Materials and General Methods. All the reagents and solvents were purchased from commercial sources and used without further purification. Solvothermal reactions were carried out in a Teflon-lined bomb reactor. The single-crystal X-ray diffraction data of *int*-MOF-5 (**1**) were collected on a ADSC Quantum 210 CCD diffractometer with synchrotron radiation at Pohang Accelerator Laboratory. The powder X-ray diffraction (PXRD) patterns were recorded on a Bruker D8 Advance system equipped with a sealed Cu tube (λ = 1.54178 Å). Thermogravimetric analysis (TGA) data were obtained on Perkin−Elmer Pyris 1 DSC and TGA instruments with a heating rate of 10 °C min^{-1} under a N_2 atmosphere. Gas sorption isotherms were volumetrically and gravimetrically recorded on the Autosorb 1MP and Robotherm MSB instruments, respectively. Highly pure gases were used for the measurements. The pH* of solutions was measured using a TOA DKK HM-30P pH meter with a GST-5721S electrode working in organic solvents. All the NMR data were recorded on a Bruker DRX400 spectrometer. The XANES and EXAFS spectra were obtained at the 10A beamline at Pohang Accelerator Laboratory.

Synthesis. *Synthesis of **1** in the Presence of Melamine.* A mixture of $Zn(NO_3)_2 \cdot 6H_2O$ (0.600 g, 2.00 mmol), H_2bdc (0.125 g, 0.75 mmol) and melamine (0.050 g, 0.38 mmol) in DMF (15 mL) was heated at 110 °C for 12 h in a Teflon-lined bomb reactor. The colorless crystalline precipitate formed were collected, washed with DMF, and dried under a reduced pressure at room temperature for 1 h (0.187 g, 76%). Anal. Calcd. for $\mathbf{1} \cdot 2.5DMF \cdot 1.5H_2O$: C, 38.62; H, 3.34; N, 3.57. Found: C, 38.63; H, 3.28; N, 3.93. ^1H NMR (400 MHz) for as-synthesized **1** digested in $NaOH/D_2O$: δ 8.42 (s, 0.3H), 7.90 (s, 2H), 7.84 (s, 12H), 2.98 (s, 6H), 2.82 (s, 6H), 2.24 (s, 1.8H). ^{13}C NMR: δ 175.25, 171.06, 164.92, 138.59, 128.51, 36.88, 36.61, 31.35.

Synthesis of ***1*** *in the Presence of Aniline.* A mixture of $Zn(NO_3)_2 \cdot 6H_2O$ (0.600 g, 2.00 mmol), H_2bdc (0.125 g, 0.75 mmol) and aniline (0.1 mL, 1.10 mmol) in DMF (15 mL) was heated at 110 °C for 12 h in a Teflon-lined bomb reactor. The colorless crystalline precipitate formed were collected, washed with DMF, and dried under a reduced pressure at room temperature for 1 h (0.196 g, 81%). Anal. Calcd. for $\mathbf{1} \cdot 2.5DMF \cdot H_2O$: C, 38.98; H, 3.27; N, 3.61. Found: C, 39.02; H, 3.45; N, 4.00. ^1H NMR (400 MHz) for as-synthesized **1** digested in $NaOH/D_2O$: δ 8.46 (s, 0.6H), 7.94 (s, 2.5H), 7.88 (s, 12H), 3.02 (s, 7.5H), 2.87 (s, 7.5H), 2.29 (s, 1.8H).

Synthesis of ***1*** *in the Presence of 2,4,6-Tri(4-pyridyl)-1,3,5-triazine.* A mixture of $Zn(NO_3)_2 \cdot 6H_2O$ (0.600 g, 2.00 mmol), 1,4-benzenedicarboxylic acid (0.125 g, 0.75 mmol), and 2,4,6-tri(4-pyridyl)-1,3,5-triazine (15 mg, 0.048 mmol) in DMF (15 mL) was heated at 110 °C for 12 h in a Teflon-lined bomb reactor. The colorless crystalline product formed was collected, washed with DMF, and dried under a reduced pressure at room temperature for 1 h (0.206 g, 80%). Anal. Calcd. for $\mathbf{1} \cdot 3.5DMF \cdot H_2O$: C, 39.70; H, 3.72; N, 4.70. Found: C, 39.62; H, 3.70; N, 4.64. ^1H NMR (400 MHz) for as-synthesized **1** digested in $NaOH/D_2O$: δ 8.45 (s, 0.2H), 7.93 (s, 2.5H), 7.87 (s, 12H), 3.01 (s, 7.5H), 2.86 (s, 7.5H), 2.28 (s, 0.6H).

Synthesis of Crystalline Materials by Adjusting the pH of Reaction Media. The pH* of a mixture of $Zn(NO_3)_2 \cdot 6H_2O$ (0.600 g, 2.00 mmol) and H_2bdc (0.125 g, 0.75 mmol) in DMF (15 mL) measured by a pH meter was 3.8. To decrease the pH* of the solution to 3.0, 2.5 M HCl solution was added, and to increase it to 5.0, 2.5 M NaOH solution was added while being carefully monitored by a pH meter (see Figure S21 in the Supporting Information). After adjusting the pH, the solutions were heated at 110 °C for 12 h in Teflon-lined bomb reactors. Colorless crystalline precipitates formed were collected, washed with DMF, and dried under a reduced pressure at room temperature for 1 h. The crystalline product obtained at pH* 4.3: Anal. Calcd. for $\mathbf{1} \cdot 2.7DMF \cdot H_2O$: C, 39.13; H, 3.37; N, 3.84. Found: C, 38.99; H, 3.51; N, 4.20.

Synthesis of MOF-5. MOF-5 was synthesized according to the literature.[24] Anal. Calcd. for $MOF\text{-}5 \cdot 9DMF \cdot 4H_2O$: C, 40.84; H, 5.58; N, 8.41. Found: C, 40.71; H, 5.90; N, 8.68.

X-ray Crystallography. The diffraction data from a colorless cubic crystal of as-synthesized **1** measuring 0.20 mm × 0.20 mm × 0.20 mm mounted on a loop were collected at 90 K on a ADSC Quantum 210 CCD diffractometer with synchrotron radiation (λ = 0.90000 Å) at Macromolecular Crystallography 6B1, Pohang Accelerator Laboratory (PAL), Pohang, Korea. The raw data were processed and scaled using the program HKL2000. The structure was solved by direct methods, and the refinements were carried out with full-matrix least-squares on F^2 with appropriate softwares implemented in SHELXTL program package. X-ray data for $\mathbf{1} \cdot 0.33DMF \cdot 0.375H_2O$: $C_{24.99}H_{15.061}N_{0.33}O_{13.705}Zn_4$, M = 800.69, trigonal, $R\bar{3}$ (No. 148), a = 18.388(3) Å, c = 43.916(9) Å, V = 12859(4) Å^3, Z = 12, T = 90 K, μ(synchrotron) = 4.255 mm^{-1}, ρ_{calc} = 1.247 g cm^{-3}, 10957 reflections measured, 4076 unique (R_{int} = 0.0602), R_1 = 0.0880, wR_1 = 0.2691 for 3941 reflections ($I > 2\sigma(I)$), R_1 = 0.0891, wR_2 = 0.2702 (all data), GOF = 1.112, 378 parameters, and 409 restraints. All the non-hydrogen atoms were refined anisotropically. Hydrogen atoms were added to their geometrically ideal positions (except for water molecules).

Gas Sorption. The hydrogen and nitrogen sorption isotherms of **1** and MOF-5 at 77 K were volumetrically measured up to 1 bar by the Autosorb 1MP instrument. The pore size distribution was obtained by Horvath−Kawazoe method from an Ar sorption experiment at 87 K. The hydrogen sorption isotherms at 77 K were also gravimetrically measured up to 100 bar, using the Robotherm MSB instrument. The buoyancies at elevated pressures were corrected by multiplying the skeleton volume of **1** and gas density at each pressure, which is provided from NIST. Total hydrogen capacities were calculated considering the pore volume (0.45 cm^3) of **1** and the bulk density of hydrogen at each pressure.

X-ray Absorption Spectroscopy. XAFS spectra of Zn K-edge for solids and solutions were measured in transmission mode at Multipole-wiggle Source BL10A (HFXAFS), Pohang Accelerator Laboratory (PAL). Reaction mixtures at pH* 3.0, 4.3, and 5.0 were prepared by adding 2.5 M NaOH or HCl, as described above,[11] and the solutions were heated at 110 °C. The reactions were monitored by XAFS at a regular interval up to 160 min. A Si(111) double-crystal monochromator was used with detuning to 60% in intensity to eliminate high-order harmonics. Energy calibration was carried out for all measurements using zinc foil placed in front of the third ion chamber. The EXAFS data were analyzed using the standard procedure in the UWXAFS software package. The normalized k^2-weighted EXAFS spectra were Fourier-transformed in the k-range from 2.8 Å^{-1} to 14.0 Å^{-1}, to show the radial distribution function of each bond pair around the central Zn atom.

■ ASSOCIATED CONTENT

Supporting Information. Experimental details for the synthesis of **1**, as well as PXRD, TGA, gas adsorption isotherms, XANES, EXAFS spectra, and enthalpy of adsorption, in addition to single-crystal X-ray data. This material is available free of charge via the Internet at http://pubs.acs.org.

■ AUTHOR INFORMATION

Corresponding Author
*E-mail: kkim@postech.ac.kr.

■ ACKNOWLEDGMENT

We gratefully acknowledge the CRI, BK21, and WCU (Project No. R31-2008-000-10059-0) Programs of MOEST, and the Steel Science Program of POSCO, for their support of this work. X-ray diffraction and XAFS studies with synchrotron radiation were performed at the Pohang Accelerator Laboratory (Beamline 6B1 and 10A, respectively) supported by MOEST and POSTECH.

■ REFERENCES

(1) Recent reviews: (a) Férey, G.; Serre, C. *Chem. Soc. Rev.* **2009**, *38*, 1380. (b) Tranchemontagne, D. J.; Mendoza-Cortés, J. L.; O'Keeffe, M.; Yaghi, O. M. *Chem. Soc. Rev.* **2009**, *38*, 1257. (c) Perry, J. J., IV; Perman, J. A.; Zaworotko, M. J. *Chem. Soc. Rev.* **2009**, *38*, 1400. (d) Kitagawa, S.; Kitaura, R.; Noro, S. *Angew. Chem., Int. Ed.* **2004**, *43*, 2334. (e) Hill, R. J.; Long, D.-L.; Champness, N. R.; Hubberstey, P.; Schröder, M. *Acc. Chem. Res.* **2005**, *38*, 337. (f) Long, J. R.; Yaghi, O. M. *Chem. Soc. Rev.* **2009**, *38*, 1213. (g) Lin, W. *MRS Bull.* **2007**, *32*, 544. (h) Wang, Z.; Cohen, S. M. *Chem. Soc. Rev.* **2009**, *38*, 1315. (i) Li, J.-R.; Kuppler, R.; Zhou, H.-C. *Chem. Soc. Rev.* **2009**, *38*, 1477. (j) Farha, O. K.; Hupp, J. T. *Acc. Chem. Res.* **2010**, *43*, 1166.

(2) (a) Lin, X.; Jia, J.; Zhao, X.; Thomas, K. M.; Blake, A. J.; Walker, G. S.; Champness, N. R.; Hubberstey, P.; Schröder, M. *Angew. Chem., Int. Ed.* **2006**, *45*, 7358. (b) Dybtsev, D. N.; Chun, H.; Yoon, S. H.; Kim, D.; Kim, K. *J. Am. Chem. Soc.* **2004**, *126*, 32. (c) Kim, H.; Samsonenko, D. G.; Yoon, M.; Hwang, Y. K.; Chang, J.-S.; Kim, K. *Chem. Commun.* **2008**, 4697. (d) Lee, J. Y.; Farha, O. K.; Roberts, J.; Scheidt, K. A.; Nguyen, S. T.; Hupp, J. T. *Chem. Soc. Rev.* **2009**, *38*, 1450. (e) Kim, K.; Banerjee, M.; Yoon, M.; Das, S. *Top. Curr. Chem.* **2010**, *293*, 115. (f) Kurmoo, M. *Chem. Soc. Rev.* **2009**, *38*, 1353. (g) Park, Y. K.; Choi, S. B.; Kim, H.; Kim, K.; Won, B.-H.; Choi, K.; Choi, J.-S.; Ahn, W.-S.; Won, N.; Kim, S.; Jung, D. H.; Choi, S.-H.; Kim, G.-H.; Cha, S.-S.; Jhon, Y. H.; Yang, J. K.; Kim, J. *Angew. Chem., Int. Ed.* **2007**, *46*, 8230. (h) Taylor-Pashow, K. M. L.; Rocca, J. D.; Xie, Z.; Tran, S.; Lin, W. *J. Am. Chem. Soc.* **2009**, *131*, 14261.

(3) (a) Batten, S. R.; Robson, R. *Angew. Chem., Int. Ed.* **1998**, *37*, 1460. (b) Reineke, T. M.; Eddaoudi, M.; Moler, D.; O'Keeffe, M.; Yaghi, O. M. *J. Am. Chem. Soc.* **2000**, *122*, 4843.

(4) (a) Maji, M. K.; Matsuda, R.; Kitagawa, S. *Nat. Mater.* **2007**, *6*, 142. (b) Ma, S.; Wang, X.-S.; Yuan, D.; Zhou, H.-C. *Angew. Chem., Int. Ed.* **2008**, *47*, 4130. (c) Kesanli, B.; Cui, Y.; Smith, M. R.; Bittner, E. W.; Bockrath, B. C.; Lin, W. *Angew. Chem., Int. Ed.* **2005**, *44*, 72.

(5) (a) Zhang, J.-J.; Wojtas, L.; Larsen, R. W.; Eddaoudi, M.; Zaworotko, M. J. *J. Am. Chem. Soc.* **2009**, *131*, 17040. (b) Shekhah, O.; Wang, H.; Paradinas, M.; Ocal, C.; Schüpbach, B.; Terfort, A.; Zacher, D.; Fischer, R. A.; Wöll, C. *Nat. Mater.* **2009**, *8*, 481. (c) Farha, O. K.; Malliakas, C. D.; Kanatzidis, M. G.; Hupp, J. *J. Am. Chem. Soc.* **2010**, *132*, 950.

(6) Farha, O. K.; Mulfort, K. L.; Thorsness, A. M.; Hupp, J. T. *J. Am. Chem. Soc.* **2008**, *130*, 8598.

(7) Li, H.; Eddaoudi, M.; O'Keeffe, M.; Yaghi, O. M. *Nature* **1999**, *402*, 276.

(8) (a) Rowsell, J. L. C.; Millward, A. R.; Park, K. S.; Yaghi, O. M. *J. Am. Chem. Soc.* **2004**, *126*, 5666. (b) Panella, B.; Hirscher, M. *Adv. Mater.* **2005**, *17*, 538. (c) Saha, D.; Deng, S.; Yang, Z. *J. Porous Mater.* **2009**, *16*, 141. (d) Petit, C.; Bandosz, T. J. *Adv. Mater.* **2009**, *21*, 4753. (e) Li, Y.; Yang, R. T. *J. Am. Chem. Soc.* **2006**, *128*, 726.

(9) Kaye, S. S.; Dailly, A.; Yaghi, O. M.; Long, J. R. *J. Am. Chem. Soc.* **2007**, *129*, 14176.

(10) Hafizovic, J.; Bjørgen, M.; Olsbye, U.; Dietzel, P. D. C.; Bordiga, S.; Prestipino, C.; Lamberti, C.; Lillerud, K. P. *J. Am. Chem. Soc.* **2007**, *129*, 3612.

(11) (a) Shen, H.; Zhang, L.; Eisenberg, A. *J. Am. Chem. Soc.* **1999**, *121*, 2728. (b) Perrin, D. D.; Dempsey, B. *Buffers for pH and metal ion control*; Chapman & Hall: London, 1974; p 77. (c) Azab, H. A.; Ahmed, I. T.; Mahmoud, M. R. *J. Chem. Eng. Data* 1995, *40*, 523. The measured pH* values do not have the same meaning as those in water. In this work, the pH* of the solution was adjusted by adding a small amount of aqueous NaOH (2.5 M) or HCl (2.5 M) solution to the reaction mixture in DMF. Throughout this work, "pH" denotes a property associated with true H^+ activity of the reaction solution, while "pH*" indicates an apparent value measured by a conventional pH meter with a glass electrode.

(12) To the best of our knowledge, the effect of pH on the synthesis of porous MOFs has not been addressed, although there are a few reports on pH-dependent assembly of nonporous coordination polymers:(a) Fang, H.-C.; Zhu, J.-Q.; Zhou, L.-J.; Jia, H.-Y.; Li, S.-S.; Gong, X.; Li, S.-B.; Cai, Y.-P.; Thallapally, P. K.; Liu, J.; Exarhos, G. J. *Cryst. Growth Des.* **2010**, *10*, 3277. (b) Meng, F.-X.; Chen, Y.-G.; Liu, H.-B.; Pang, H.-J; Shi, D.-M; Sun, Y. *J. Mol. Struct.* **2007**, *837*, 224.

(13) The space group of **1** was previously reported as $R\bar{3}m$. However, the high symmetry group did not allow us to locate guest molecules in the pores. Subsequently, the symmetry was reduced to $R\bar{3}$ to locate the guest molecules in the difference electron density map. See SI1 in the Supporting Information for details.

(14) Spek, A. L. *PLATON, a multipurpose crystallographic tool*; Utrecht University: Utrecht, The Netherlands, 2001.

(15) The MOF-5 sample might be contaminated with a small amount of **1**, as suggested by its DSC data (see Figure S5 in the Supporting Information).

(16) Introduction of a small amount of water (up to 0.63%) to the reaction mixture was inevitable as aqueous NaOH/HCl solution was used when the pH* was adjusted. The addition of a small amount of water to the reaction mixture seemed to affect the product distribution but did not facilitate the formation of phase-pure **1** (see Figure S9 in the Supporting Information).

(17) (a) Hawxwell, S. M.; Adams, H.; Brammer, L. *Acta Crystallogr., Sect. B: Struct. Sci.* **2006**, *62*, 808. (b) Liao, J.-H.; Lee, T.-J.; Su, C.-T. *Inorg. Chem. Commun.* **2006**, *9*, 201.

(18) Surblé, S.; Millange, F.; Serre, C.; Férey, G.; Walton, R. I. *Chem. Commun.* **2006**, 1518.

(19) Ozutsumi, K.; Koide, M.; Suzuki, H.; Ishiguro, S.-i. *J. Phys. Chem.* **1993**, *97*, 500.

(20) High hydrogen sorption capacities of MOFs were reported. See the following examples:(a) Lin, X.; Jia, J.; Zhao, X.; Thomas, M.; Blake, A. J.; Walker, G. S.; Champness, N. R.; Hubberstry, P.; Schröder *Angew. Chem., Int. Ed.* **2006**, *45*, 7358. (b) Koh, K.; Wong-Foy, A. G.; Matzger, A. J. *J. Am. Chem. Soc.* **2009**, *131*, 4184.

(21) Crystallographic densities of guest-free **1** (1.193 g cm^{-3}) and MOF-5 (0.595 g cm^{-3}) were used to calculate the volumetric hydrogen uptakes.

(22) Rowsell, J. L. C.; Yaghi, O. M. *J. Am. Chem. Soc.* **2006**, *128*, 1304.

(23) Wong-Foy, A. G.; Matzger, A. J.; Yaghi, O. M. *J. Am. Chem. Soc.* **2006**, *128*, 3494.

(24) Eddaoudi, M.; Kim, J.; Rosi, N.; Vodak, D.; Wachter, J.; O'Keeffe, M.; Yaghi, O. M. *Science* **2002**, *295*, 469.